APPLICATION OF RIGOROUS INTEGRATED PRODUCTION MODELLING METHODS TO GREATER WESTERN FLANK GAS FIELD DEVELOPMENT

N.J. Hawkes[1], P.F. Pickering[1], C.E. Butler[2], M.B. Brown[2], and S.M. Thomson[3]

[1] FEESA Ltd, Farnborough, UK; [2] Woodside Energy Ltd, Perth, Australia;
[3] Xodus Pty Ltd, Perth, Australia

ABSTRACT

The paper describes the application of rigorous integrated production modelling (IPM) methods to the Greater Western Flank development on the North West Shelf Venture (NWSV), operated by Woodside Energy Ltd. The development comprises up to nineteen discrete gas accumulations to be developed by tying back to existing infrastructure. The objective of the work was to simulate different facility configurations, in order to identify the best technical and economic solutions. Simulation models were developed for predicting life-cycle production rates. The models included the existing infrastructure, and therefore properly quantified the hydrodynamic interaction between new and producing fields. In addition, logical rules were embedded to provide intelligent field sequencing, optimal allocation, automatic abandonment, and several other physical constraints. Furthermore, the models had rigorous physical bases, incorporating compositional mixing, phase equilibrium and gas-liquid multiphase flow models. As a result, it was possible to screen simultaneously for steady state operational issues, such as liquid accumulation in pipelines and hydrate avoidance. An example production profile is presented showing how new fields are sequenced to maintain feed rates to the shore-based LNG plant. In addition, phase diagrams are given showing the different phase behaviour predicted and the effect this could have on system operation, especially from the point of view of hydrate avoidance. Liquid holdup characteristics are also given for an example pipeline at different liquid loadings. It is concluded that rigorous IPM offers numerous advantages during field development planning by allowing different options to be screened for economic and technical feasibility simultaneously. This reduces the design time and leads to more optimal designs.

INTRODUCTION

As the global quest for offshore hydrocarbon production advances, the definition of viable projects becomes increasingly more challenging for a variety of reasons, such as deeper waters or harsher environments. In addition, in maturing provinces the challenge is often to recover reserves from multiple small fields, where individually fields are uneconomic, but when brought together in a common production infrastructure, viable projects can be defined.

However, where multiple fields produce through a common system, their mutual interactions influence the production rates, which affects the revenue stream and, hence, the project economics. Therefore, the designer is faced with the difficult problem of quantifying the interactions. Moreover, with these systems, there are usually numerous technical challenges that must be surmounted if uninterrupted production is to be maintained. In gas systems, as described here, these include avoiding blockages due to hydrates, controlling system integrity in the face of erosion-corrosion effects and managing liquid inventories that accumulate in pipelines. Any of these *flow assurance* problems can stymie production or even render systems inoperable and, preferably, they should be designed out at an early stage. Furthermore, since economic feasibility is strongly governed by the achievable production rates and revenues, reliable prediction of system deliverability is the *sine qua non* of good design.

This paper describes the application of rigorous integrated production modelling (IPM) methods to the NWSV Greater Western Flank (GWF) development. This is a large multi-field gas development located on the Australian North-West Shelf, nearby to the existing Goodwyn and North Rankin facilities. The scope of the GWF development is wide-ranging, comprising of up to nineteen new accumulations to be tied back to the existing infrastructure. The principal objective of this work was to simulate different facility configurations in order to identify the best technical and economic solutions.

METHODOLOGY

Integrated Production Modelling

The term "integrated production modelling" (IPM), refers to models comprising all elements from the underground hydrocarbon reservoirs to the point of delivery. For these systems, the natural boundary conditions are the pressures existing in the reservoirs and at delivery. Given these boundary conditions, and mathematical models for the wells, flowlines, risers and processing equipment forming the production systems, it is possible to solve for the production rates throughout the system. If the production rates are predicted through the life of a development, a production forecast can be constructed. This forecast then provides the revenues for economic evaluation; the central objective of IPM.

The IPM tool used in this study is called *Maximus*. This tool is described in an accompanying paper (Pickering *et al*, 2009) and two earlier papers (Watson *et al*, 2006 & 2008). The method of solution is founded on the *Equation Oriented* approach, first developed for process analysis (Sargent and Westerberg, 1964 and Pantelides, 1988).

Physical Models of Greater Western Flank

Figure 1 presents a schematic of the GWF dual pipeline model. Wells in the GWF development are shown on the left-hand side of the figure. This scheme envisages collecting the GWF volumes via dual subsea production pipelines. For this specific layout, the Southern and Northern pipelines are circa 65 km and 35 km in length, respectively.

The gas from GWF arrives at the existing Goodwyn A platform where it is processed before being dispatched through the interfield pipeline to the North Rankin facilities. If the GWF gas is at pressures sufficient for onward transportation without compression, then it passes through the T100 bypass receiving only dehydration. However, if the gas is at lower pressures, insufficient for onward shipping at the required rates, it is passed through the existing T200 compressor before export. On the Goodwyn A platform the GWF gas is also commingled with gas from the currently producing Goodwyn and Perseus fields. On arrival at the North Rankin facilities, the production from Goodwyn A is joined by production from North Rankin A and other facilities, before entering the twin trunklines for final transport the 134 km to shore.

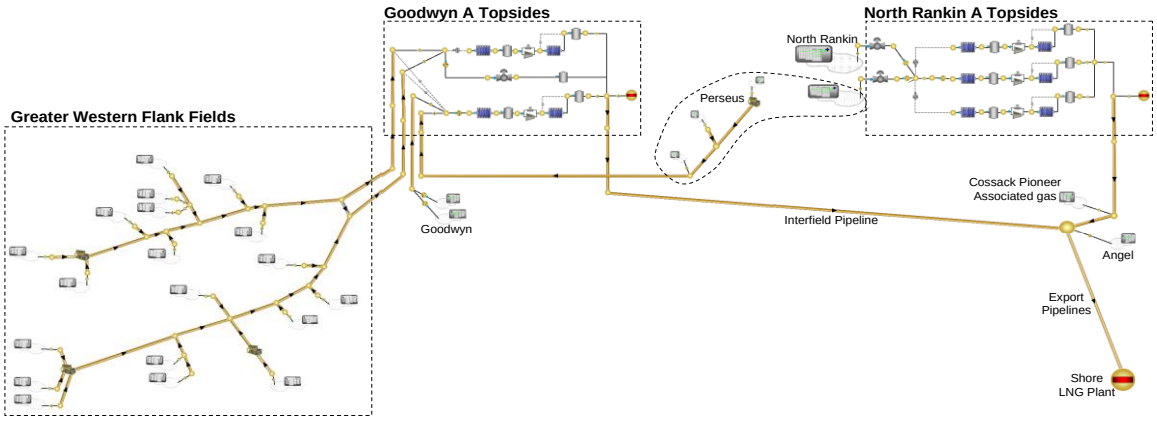

Fig. 1: Schematic of Greater Western Flank Dual Pipeline Model

Another concept being considered envisages a new platform for GWF gas compression, as shown in Figure 2. For this concept, several of the GWF wells are drilled directly from the new platform with the remaining tied in through a subsea pipeline.

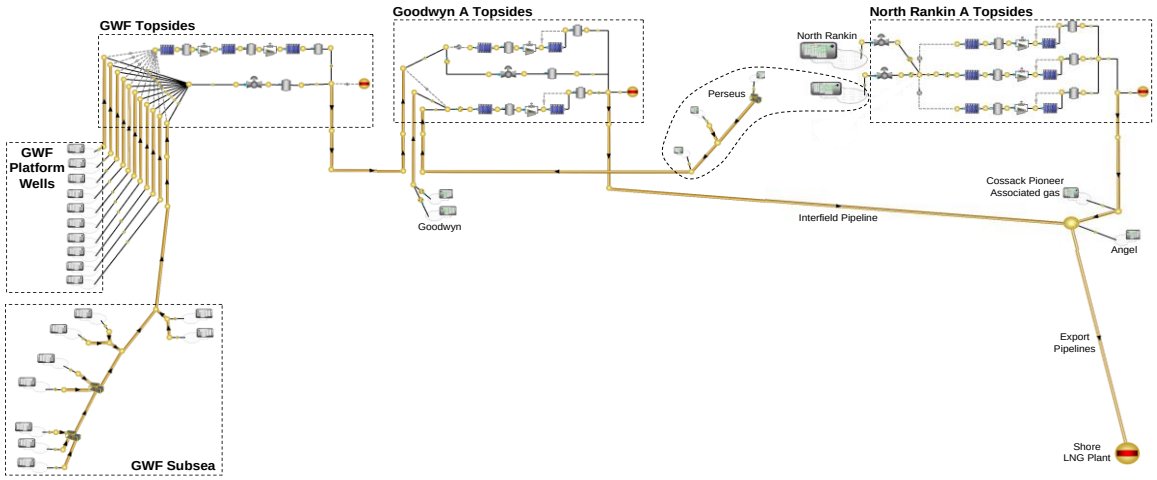

Fig. 2: Schematic of Greater Western Flank Infield Compression Model

Details of how models like those in Figures 1 and 2 are solved, are given in the accompanying paper (Pickering *et al*, 2009).

Reservoir Modelling

The reservoir modelling followed a multidimensional table approach based on the typecurve data format that Woodside uses when generating integrated NWSV production forecasts. These data were generated for each accumulation, at a range of wellhead pressures, using reservoir simulator or Equation of State models. These were closed with top-hole boundary pressures and contained sub-models describing the behaviour of the reservoir, pressure losses in the near well regions (also referred to as inflow performance) and the production wells. A segment of typecurve data (as input to the IPM tool) is shown in Table 1 for a specific top-hole pressure boundary condition. The independent variable, given in the first column, is the total cumulative gas production. The other columns are dependent variables, giving the cumulative amounts of various components and the mass flowrate potential. At a given total cumulative gas, the corresponding mass flowrate potential gives the maximum production rate achievable with the specified top-hole pressure boundary condition. In addition, the cumulative amounts for the individual components allow the composition of the gas to be derived for a given total cumulative gas.

Cumulative Gas	Nitrogen	Carbon Dioxide	Methane	Ethane	Propane	N-Butane	C5P	Water	Mass Flowrate
Active	Active	Active	Active	Active	Active	Active	Active	Active	Active
Msm3	kg	kg	kg	kg	kg	kg	kg	kg	kg/s
0	0	0	0	0	0	0	0	0	264
159	2702080	4786130	87673800	13654100	9845340	6827060	32487300	1488905	261
317	5376850	9523890	174462000	27170300	19591200	13585100	64797300	2967365	258
473	8024840	14214200	260380000	40551100	29239400	20275500	96931900	4435596	256
627	10646500	18857900	345446000	53798900	38791800	26899500	128892000	5893783	253
780	13242400	23456000	429675000	66916500	48250300	33458300	160681000	7342167	251
932	15813000	28009200	513082000	79906300	57616600	39953100	192299000	8780926	248
1082	18358700	32518400	595682000	92770100	66892100	46385100	223748000	10210191	246
1230	20880000	36984200	677489000	105511000	76078700	52755300	255029000	11630271	244
1378	23377300	41407600	758518000	118130000	85177900	59065000	286144000	13041213	241
1524	25859100	45799400	839004000	130654000	94202600	65316200	316737000	14446138	239

Tab. 1: Section through Typical Table of Typecurve Data

To complete a reservoir's typecurve data, multiple tables (such as that pictured in Table 1) must be provided for a range of top-hole pressures. Thus, for a particular total cumulative gas production, it is then possible to represent the performance of the reservoir in terms of the top-hole pressure and the flowrate.

Figure 3a shows the variation of flowrate potential with total cumulative gas production for a reservoir. The graph includes a family of curves where each was predicted for a given top-hole pressure boundary condition. The curve that intercepts the ordinate axis at the largest value of mass flowrate (~260 kg/s) corresponds to the smallest pressure and the one that intercepts at the smallest value (~50 kg/s) corresponds to the largest pressure. The functional dependence of top-hole pressure P on flowrate Q, at a given cumulative gas, is shown in Figure 3b. Referred to as a "PQ curve", the dependency resembles an elliptic quadrant. As the cumulative gas production increases the reservoir pressure reduces and the prevailing PQ curve collapses towards the origin as shown.

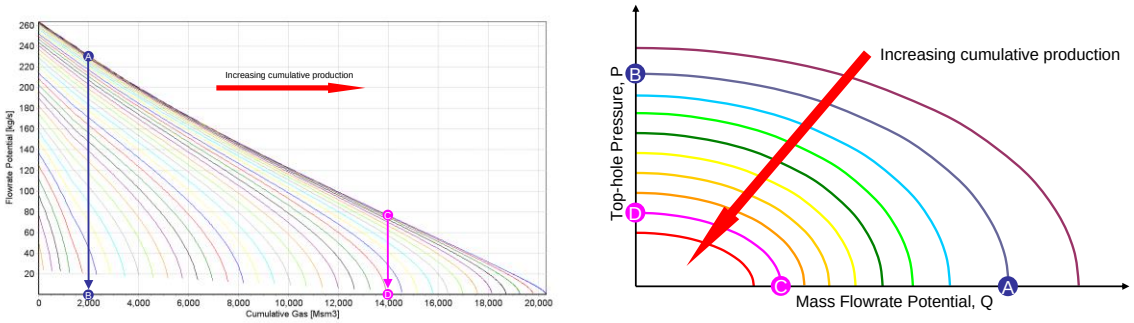

(a) Potential versus Cumulative Gas *(b) PQ Curves*

Fig. 3: Typecurve Flowrate Potential with Top-hole Pressure

In solving a network problem with the reservoirs defined using typecurves, the problem is closed with PQ curve boundary conditions rather than simple pressure or flowrate specifications. In addition, the typecurve data describing the variations of the individual components are used to determine instantaneous compositions. This allows the compositional variations that occur as the reservoir pressure reduces to be captured.

Thermophysical Properties and Phase Behaviour

All calculations were performed using compositional descriptions of the reservoir fluids, with the set of components: nitrogen, carbon dioxide, methane, ethane, propane, butanes and water. Hydrocarbon components at C_5 and higher were modelled with the plus fraction C_{5+}. Variations in reservoir fluid compositions through field life were captured in the typecurve data, thus replicating the important observed effects of 'leaning out' and 'watering out'. These effects are illustrated in Figure 4.

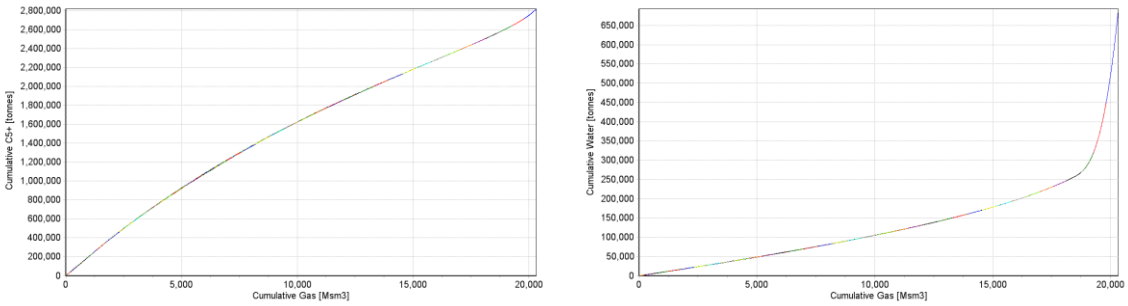

(a) C5+ Component *(b) Water Component*

Fig. 4: Compositional Variations with Cumulative Gas

The expression 'leaning out' refers to the reduction in natural gas liquids (NGLs) in the produced gas due to *retrograde condensation* in the reservoir (Bradley *et al*, 1987 or Ahmed, 1989). The rate of production of C_{5+}, which is a measure of the NGLs produced, is given by the gradient of the curve depicted in Figure 4a. From left to right it can be seen that the gradient reduces continuously, until the curve passes through an inflection, when it increases again. Hence, for this reservoir, the proportion of C_{5+} in the produced gas, and therefore the amount of NGLs, passes through a minimum.

Natural gas wells may also 'water out' due to ingress of formation water from a nearby mobile aquifer. In Figure 4b, watering out occurs towards the right-hand side of the graph where there is a sharp change in the gradient. The comparatively small increases in the gradient (and water content) prior to this arise due to the depressurisation of the reservoir and the corresponding evaporation of some static connate water.

Further explanation of the compositional changes occurring in produced natural gas is given by the example phase diagram in Figure 5. This diagram shows six regions where different combinations of four phases coexist: hydrocarbon vapour (V), hydrocarbon liquid (HL), aqueous liquid (AL) and hydrate II (HII). From the diagram, the hydrocarbon dewpoint, water saturation and hydrate curves are evident. Also shown inside the phase envelope are the constant quality lines in the range 75-95%.

The locus shown as A→B→C→D traces an isothermal path as the reservoir pressure decreases. Point A is above the dewpoint curve and all of the hydrocarbon liquids are in the gas phase. However, as the pressure reduces the dewpoint is reached and hydrocarbon liquid begins to condense. At point B, the water saturation line is traversed and all of the liquid water present is now in the gas phase. As the pressure is lowered still further, more hydrocarbon liquid is formed, until point C is reached and the retrograde condensation region finishes. At pressures lower than point C, the hydrocarbon liquids evaporate progressively and the gas becomes richer in NGLs.

These compositional effects occurring through field life might seem, at first sight, esoteric and irrelevant to the problem in hand. However, these effects are actually quite significant. First, as the NGLs represent a significant revenue stream, their correct prediction is important for the economics. Second, the correct prediction of liquids rates (both NGLs and water) through the systems is imperative for various steady state *flow assurance* assessments, including liquid holdup and hydrate inhibitor calculations.

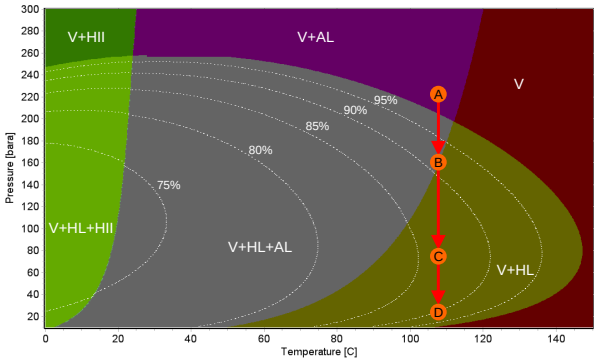

Fig. 5: Phase Diagram for Typical Reservoir Gas

Heuristic Optimisation

The previous sections have described the physical modelling of network problems, identifying the key aspects necessary for solving for the flow distribution with appropriate boundary conditions. However, the discussion has yet to cast light on how the problem of designing the GWF production systems might be solved. This is, in essence, a techno-economic optimisation problem where one seeks to discover the 'best' economic solution, satisfying all physical and commercial constraints, from a myriad of possibilities. The first step in this optimisation is to define an *objective function* to be maximised. A popular choice in production optimisation problems, is the instantaneous revenue, which is then maximised using predefined adjustable parameters:

$$\underset{\underline{x}\in X}{\text{Max}}\left[\sum_{i}\rho_i(t)Q_i(\underline{x},t)\right]$$

Where ρ_i and Q_i are the price and flowrate of product i respectively and $\underline{x}$ is a vector of adjustable parameters. This function can be maximised, in one way or another, to give the values in $\underline{x}$ that confer the maximum instantaneous revenue. However, for the GWF design problem, the task is not to locate the instantaneous optimum, but rather to identify the most economic solution. Therefore, more appropriate objective functions would be the Net Present Value (NPV), the Internal Rate of Return (IRR) or perhaps the Total Revenue (TR). In the case of the TR, the objective function now becomes:

$$\underset{\underline{x}\in X}{\text{Max}}\left[\int_0^{\tau}\sum_{i}\rho_i(t)Q_i(\underline{x},t)dt\right]$$

The integral is over the anticipated duration of field life τ. To perform this optimisation rigorously, for any except the most trivial problems, would be very difficult indeed, for not only is the number of adjustable parameters very large, the nature and structure of the problem changes as new fields commence production or as different routing options are selected. Hence, the integral is not continuous across the domain. To simplify the problem, while still achieving a rigorous optimisation, it is tempting to consider whether the maximisation and integral operators can be commuted, based on the supposition that the integral of the maximised function equals the maximum of the integral function. Alas, this is unlikely to be true because the way a reservoir is produced today will affect its ability to produce in the future. Hence, the instantaneous optimum will not usually coincide with the long-term one.

These difficulties, together with current computing limitations, effectively render rigorous optimisation intractable. Therefore, the approach adopted here employs a trial and error solution where each integration through field life obeys a set of heuristic optimisation rules.

The set of rules was defined to: (a) maintain the total gas production rate to meet the target rate for the shore-based LNG plant; (b) produce from richer fields with preference to leaner fields to maximise production of NGLs; (c) defer capital expenditure by delaying the drilling of new GWF fields for as long as possible; and (d) order new GWF fields intelligently to use the better fields first.

RESULTS AND DISCUSSION

Ordering of New Fields

The GWF fields were divided into groups based on several factors, including location of tie in to production system, access to compression and field maturity. The sequence of fields within a specific group was then determined by the IPM tool. The simulation triggered all fields in a given group before moving on to fields in the next specified group. Within a group, the choice between competing new fields was performed using automatic heuristic rules, making the selection objective. For ordering new fields, three rules were investigated based on the: (a) maximum flowrate potential; (b) maximum ultimate recovery; and (c) maximum value function. Rules (a) and (b) are fairly self-explanatory. However, the maximum value function requires some explanation. This function was derived by assuming that, for comparison purposes, new fields produce approximately linearly, with an initial flowrate of $Q_i(t_0)$, but declining to zero when the recoverable reserves R_i have been produced (where the subscript now refers to field i). The incremental value δV_i produced in time interval δt is given by:

$$\delta V_i(t) = \rho_i(t) Q_i(t) D(t) \delta t$$

Where $\rho_i(t)$ and Q_i are the price and flowrate of product from field i respectively and D(t) is a continuous value discount function taking account of the time value of money. If this expression is integrated from t_0 through to the end of production for field i, then the resulting value function is given by:

$$V_i = \frac{\rho_i Q_i(t_0)}{\ln|1+r|}\left[1 - \frac{Q_i(t_0)}{2R_i \ln|1+r|}\left(1 - e^{-2R_i \ln|1+r|/Q_i(t_0)}\right)\right]$$

Where r is the annual discount fraction. Clearly, this expression is based on certain assumptions which are unlikely to hold true exactly. However, the function is intended to provide a comparative measure suitable for ranking new fields and deciding which to start up next. Therefore, its basis is as equally valid as the other two ranking functions: (a) maximum flowrate potential $Q_i(t_0)$ and (b) maximum ultimate recovery R_i.

Figure 6 shows an example production profile for the entire NWSV. Production from the GWF fields commences shortly after the first year. The new fields are then brought on automatically, based on the user-defined heuristic rules, to maintain the total field production. The step at 2 years occurs because of a change to the specified total rate.

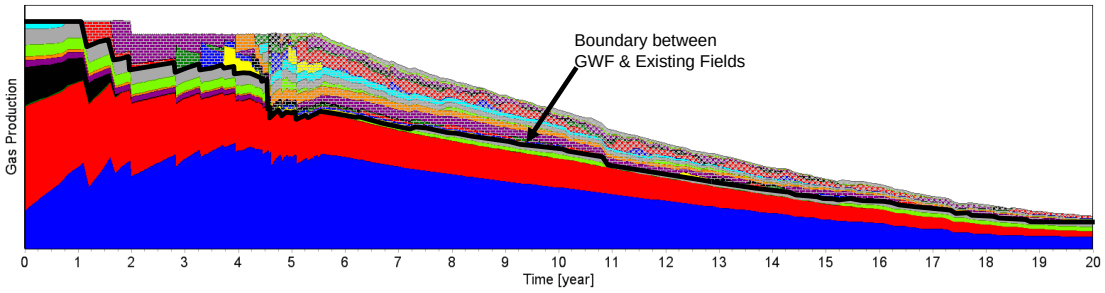

Fig. 6: Example GWF Production Profile for Dual Pipeline Case

For this case, the ordering of new fields was determined using the maximum flowrate potential. Analogous simulations were performed using the other two heuristics; a comparison between them is made in Figure 7. The results show the build-up in the number of GWF wells, which is an indicator of the phasing of development CAPEX. The graph indicates a slightly improved CAPEX profile with the maximum ultimate recovery and the maximum value function methods. But since the maximum ultimate recovery rule is simpler to implement, this would appear to have the greater utility.

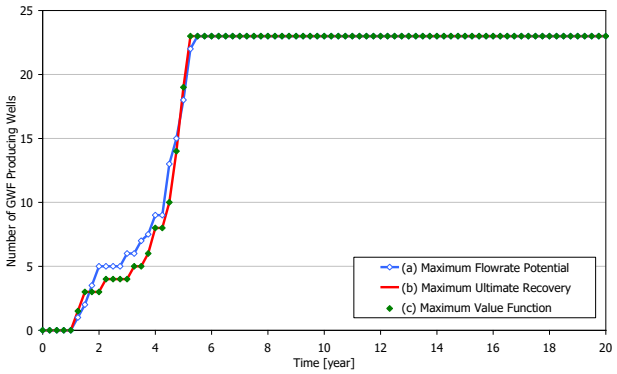

Fig. 7: Well Build-up Profile for Different Start-up Rules

Steady State Flow Assurance

A novel aspect of the work described here is that several flow assurance constraints were tested simultaneously with the IPM calculations. In particular, because the thermophysical properties and phase behaviour were determined using rigorous, thermodynamically consistent, compositional methods, it was possible to check the pressure-temperature (pT) predictions throughout the pipeline network and through field life against compatible and accurate phase diagrams. Figure 8a shows a phase diagram generated for the initial fluid composition entering the Southern pipeline in the GWF dual pipeline case (Figure 1). Overlaid are two pT profiles for the first section of the same pipeline. Initially, the gas flowrate is quite high, leading to a significant pressure drop with only a modest temperature drop. However, later, when the flowrate has reduced, the pipeline is effectively isobaric and the temperature decreases near to the ambient value. Both these pT profiles avoid the hydrate envelope, indicating that hydrates are unlikely during steady state conditions, in this case. Alternatively, Figure 8b shows the end temperature and start pressure as functions of time. These data can also be used to assess hydrate risk under steady conditions.

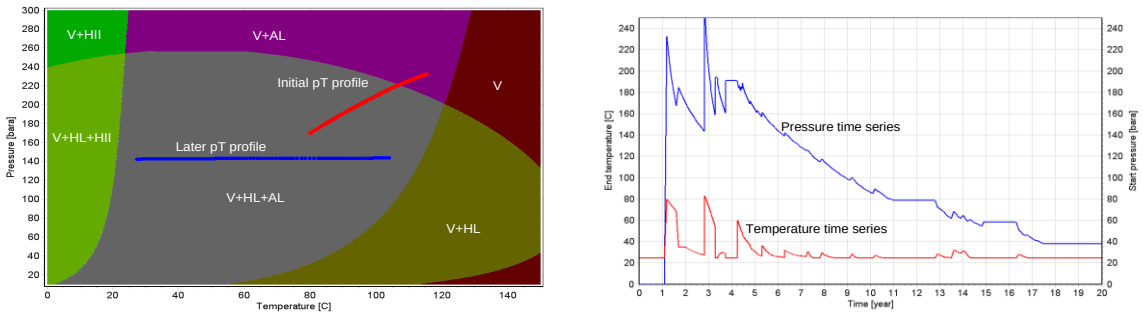

(a) Phase Diagram & pT Profiles *(b) Pipeline p & T versus Time*

Fig. 8: Pipeline Hydrate Avoidance

In addition, sensitivity calculations were performed to assess levels of liquid accumulation and the ramifications regarding operation. Figure 9 presents example liquid holdup characteristics for the pipeline section referred to above. The calculations were performed using a Taitel and

Dukler based model (Taitel & Dukler, 1976) with closure relationships based on those proposed by Bendiksen *et al* (1991).

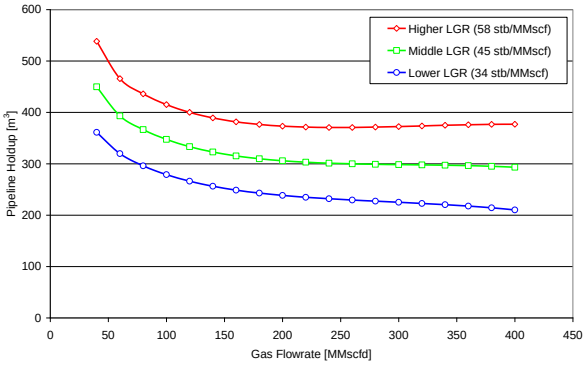

Fig. 9: Pipeline Liquid Holdup Parametrics

The results illustrate the familiar form of the liquid holdup-flowrate curve, with the pipeline accumulating liquid at reduced flowrates. This phenomenon is important because when the flowrate is restored to the normal operating rate, the accumulated liquids are produced to the reception facilities and may exceed liquids handling capacities. Therefore, the calculation of holdup characteristics is useful in the assessment of liquids management issues.

CONCLUSIONS

The work described here applied rigorous integrated production modelling or "RIPM" to the screening of different options for the Greater Western Flank gas development. The models encompassed the entire NWSV offshore facilities, including the existing facilities. Hence, it was possible to quantify the interactions between the old and the new fields. Intelligent user-defined heuristic rules were also applied to ensure efficient start up of new fields and, therefore, use of CAPEX. The models were also used to screen for several flow assurance issues, such as liquids management in pipelines and hydrate avoidance. It is concluded that RIPM offers numerous advantages during field development planning by allowing different options to be screened for economic and technical feasibility simultaneously. This reduces the design time and leads to more optimal designs.

ACKNOWLEDGEMENTS

We are grateful to BHP Billiton Petroleum (North West Shelf) Pty Ltd, Shell Developments Australia Pty Ltd, Japan Australia LNG (MIMI) Pty Ltd, BP Developments Australia Pty Ltd, Chevron Australia Pty Ltd for approval to publish.

REFERENCES

Ahmed T. 1989, Hydrocarbon Phase Behavior, Contributions in Petroleum Geology & Engineering, Volume 7, Gulf Publishing Company.

Bendiksen K.H., D. Malnes, R. Moe and S. Nuland 1991, The Dynamic Two-Fluid Model OLGA: Theory and Application, SPE Production Engineering, SPE 19451, pp. 171-180.

Bradley H.B. *et al* 1987, Petroleum Engineering Handbook, Society of Petroleum Engineers, Richardson, Texas, US.

Pantelides C.C. 1988, Speed-Up – Recent Advances in Process Simulation, Comp. & Chem. Eng., Vol. 12, pp. 745-755.

Pickering P.F., N.J. Hawkes and M.J. Watson 2009, Application of Chemical Engineering Methods to Integrated Production Modelling, Chemeca 2009 Conference, 27-30 September 2009, Burswood Entertainment Complex, Perth, Australia.

Sargent R.W.H. and A.W. Westerberg, 1964, SPEED-UP in Chemical Engineering Design, Trans. Inst, Chem. Eng., Vol. 42, pp. 190-197.

Taitel Y. and A.E. Dukler 1976, A Model for Predicting Flow Regime Transitions in Horizontal and Near Horizontal Gas-Liquid Flow, AIChE J., Vol. 22, No. 1, pp. 47-55.

Watson M.J., N.J. Hawkes, P.F. Pickering, J. Elliott and L.W. Studd, 2007, Integrated Flow Assurance Modelling of the BP Angola Block 18 Western Area Development, SPE Projects, Facilities & Construction, June 2007, SPE 101826.

Watson M.J., N.J. Hawkes, P.F. Pickering and L.D. Brown 2008, Efficient Conceptual Design of an Offshore Gas Gathering Network, 2008 SPE Asia Pacific Oil & Gas Conference and Exhibition held in Perth, Australia, 20–22 October 2008, SPE 116593.